Simulating 'Macroscopic' Dynamics in Magnetically Confined Plasmas: an overview of the NIMROD project

Carl Sovinec

University of Wisconsin-Madison

Department of Engineering Physics

UW Plasma Seminar

October 29, 2007

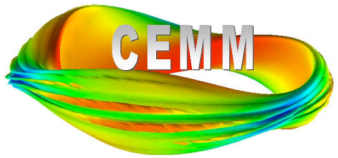

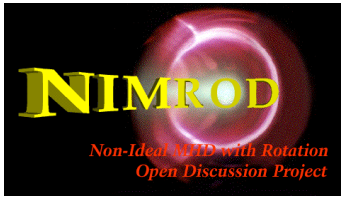

Acknowledgments

The NIMROD Team:
R. A. Bayliss, D. D. Schnack, and P. Zhu, *Univ. of Wisconsin-Madison*
S. E. Kruger, *Tech-X Corporation*
E. D. Held and J.-Y. Ji, *Utah State University*
C. C. Kim, *University of Washington*
D. P. Brennan, *University of Tulsa*
D. C. Barnes and S. E. Parker, *University of Colorado at Boulder*
V. A. Izzo, *General Atomics Corporation*
A. Y. Pankin, *Lehigh University*

TOPS Collaborators:
X. Li, *Lawrence-Berkeley National Laboratory*
D. K. Kaushik, *Argonne National Laboratory*

CEMM Collaboration (headed by)
S. Jardin, *Princeton Plasma Physics Laboratory*

Outline

- Project objectives
- Macroscopic plasma dynamics
  - Characteristics
  - Current applications
- PDE system
- Computational modeling
  - Numerical methods
    - High-order spatial representation
    - Time-advance for drift effects
  - Implementation
- Conclusions

NIMROD, Non-Ideal Mhd with Rotation, Open Discussion Project Objectives

- Produce a code for simulating macroscopic dynamics in high-performance tokamaks.
- Make the tool sufficiently general for a wide variety of alternate concepts.
- Allow flexibility for modeling different effects:
  - Two-fluid modeling
  - Neoclassical closures
  - Fast-particle interaction
- Make the software available to fusion-community users.

As we approach conditions for ignition, where new nonlinear effects may exist, the need for predictive simulation increases.

Critical 'macroscopic' topics include:

1. Internal kink stability
2. Neoclassical tearing excitation and control
3. Edge localized mode control
4. Wall-mode feedback

[2002 Snowmass Fusion Summer Study]

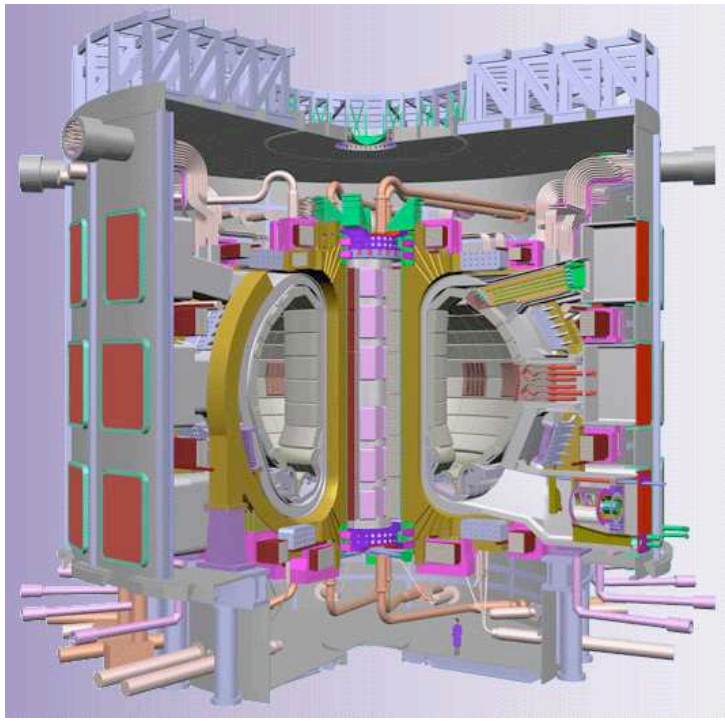

Under construction in France: International Thermonuclear Experimental Reactor (ITER)

- Fusion power: 500 MW
- Stored thermal energy: 10s of MJ

Macroscopic Plasma Dynamics

- **Magnetohydrodynamic (MHD) or MHD-like activity limits operation or affects performance in almost all magnetically confined configurations.**
- **Analytical theory has teaches us which physical effects are important and how they can be described mathematically.**
- **Understanding consequences in experiments (and predicting future experiments) requires numerical simulation:**
    - **Sensitivity to equilibrium profiles and geometry**
    - **Strong nonlinear effects**
    - **Competition among physical effects**

The physics of interest includes substantial ranges of the temporal and spatial scales found in magnetized plasmas.

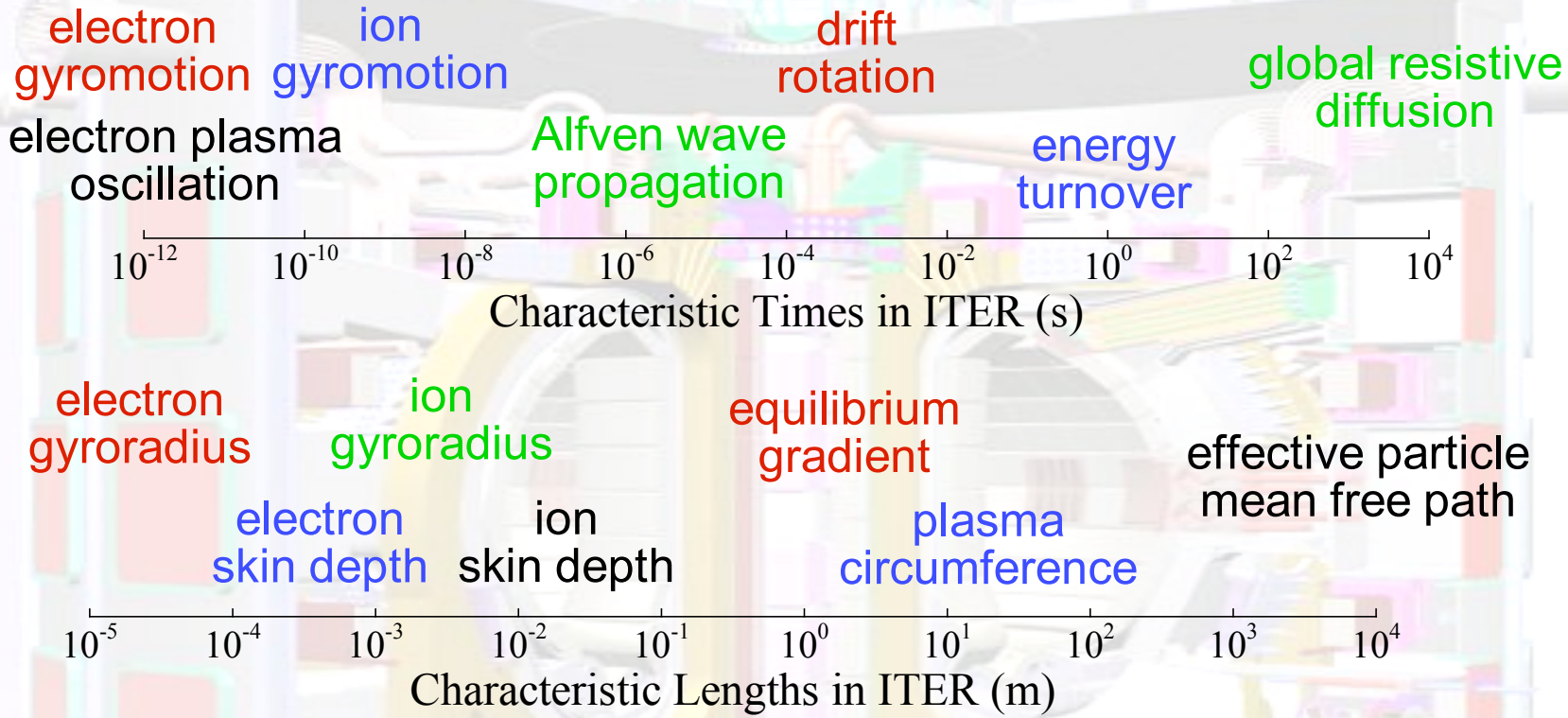

- Magnetic reconnection occurs at electron spatial scales and influences modes that extend over the device.
- Dynamical evolution may be as slow as the energy turnover time while depending on the equilibration of MHD and two-fluid propagation.
- The current applications explore different effects in isolation and in combination.

Current application areas: interchange

- Analysis of nonlinear MHD ballooning has clarified where explosive growth is possible. [Zhu]
- Classical slab interchange has been used to benchmark two-fluid stabilization and investigate gyroviscous effects. [Schnack, Zhu, Ebrahimi, and Suzuki]
- Nonlinear interchange computations consider filament formation in MHD and two-fluid modeling. [Zhu]
- Nonlinear cylindrical interchange extends earlier slab results on current-sheet formation. [Zhu]
- ELM computations for OFES office-wide performance targets for FY05-06 culminated in two-fluid simulation in realistic geometry.
- ELM modeling for ITER and FSP. [Pankin, Lehigh]

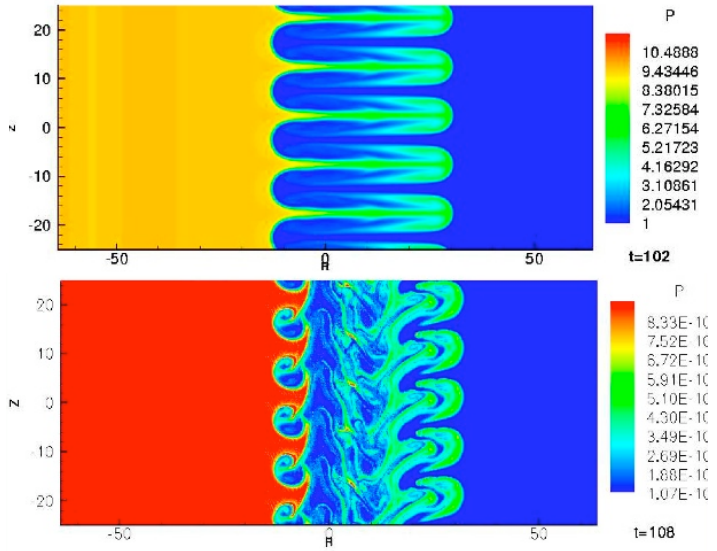

Comparison of MHD (top) and two-fluid (bottom) nonlinear interchange evolution.

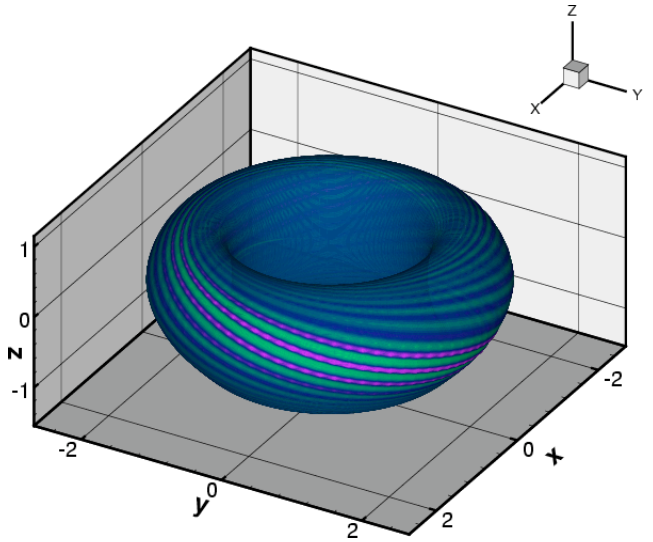

Temperature perturbations from a nonlinear two-fluid ELM simulation.

Application areas: magnetic reconnection

- Linear two-fluid benchmarking with analytical results in slab and cylindrical geometry. [King]
- GEM computations for nonlinear two-fluid benchmarking and weak guide-field studies. [U-WI]
- Nonlinear island evolution and two-fluid dynamo effect. [King]
- Two-fluid MRX simulation. [Murphy--also see CMSO applications]
- Two-fluid tearing with large ion-orbit kinetics. [Kim, U-WA]
- Tokamak sawtooth simulation with MHD and two-fluid modeling. [U-WI and Tech-X]

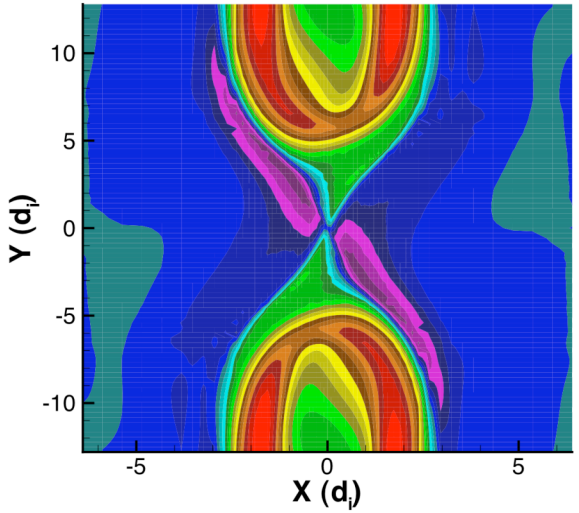

Out-of-plane magnetic field for two-fluid GEM evolution with B_{guide} equal to B_{rec}.

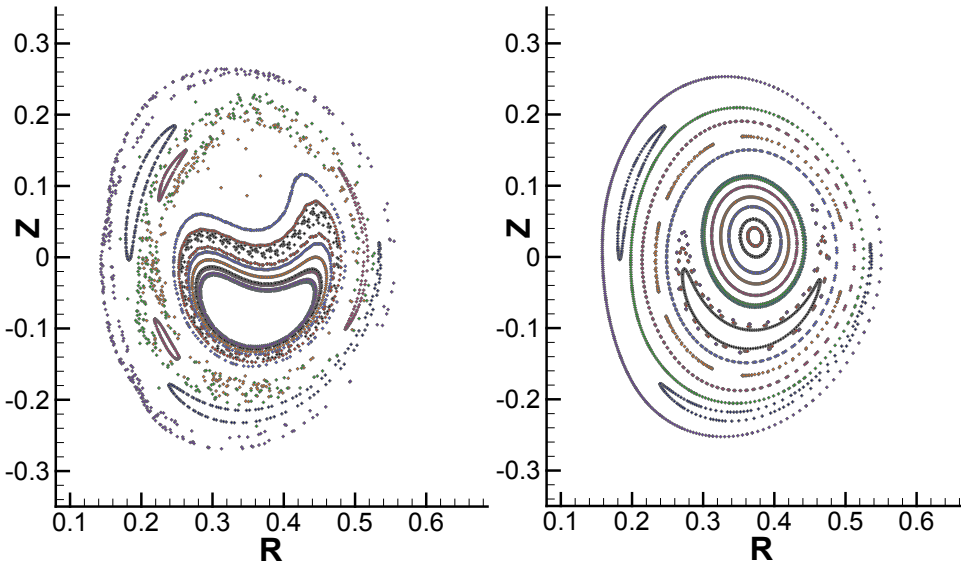

Poincare surfaces of section showing crash and recovery phases of nonlinear CDX-U benchmark with M3D.

Application areas: other large tokamak

- Disruption mitigation studies investigate important MHD mixing effects, now including impurity radiation modeling. [Izzo, GA/UCSD]
- Resonant magnetic perturbation studies. [Izzo, GA; Kruger, Tech-X]
- Tokamak island evolution simulation with RF/NTM modeling for SWIM. [Jenkins and Schnack, U-WI; Held and Ji, USU]
- A proposed study will consider energetic particle effects on tokamak 2/1 island evolution. [Brennan, U-Tulsa]

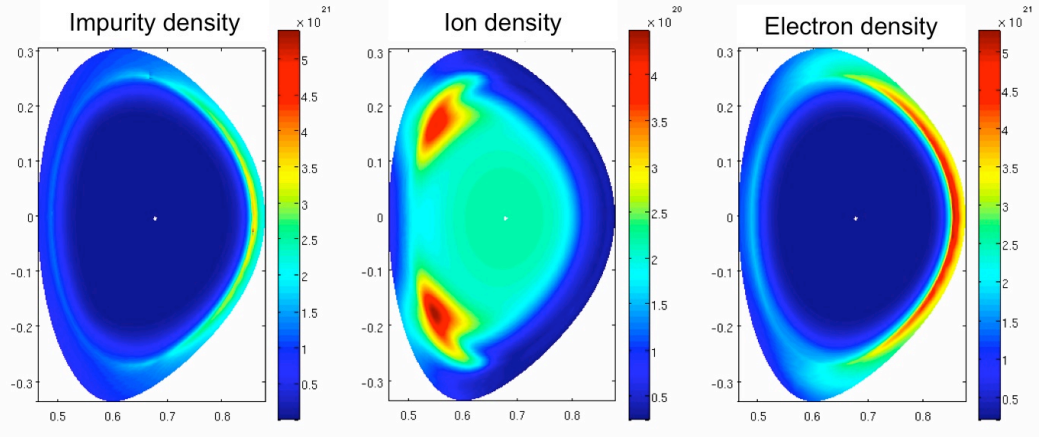

Radiation modeling with the KPRAD code uses three separate densities.

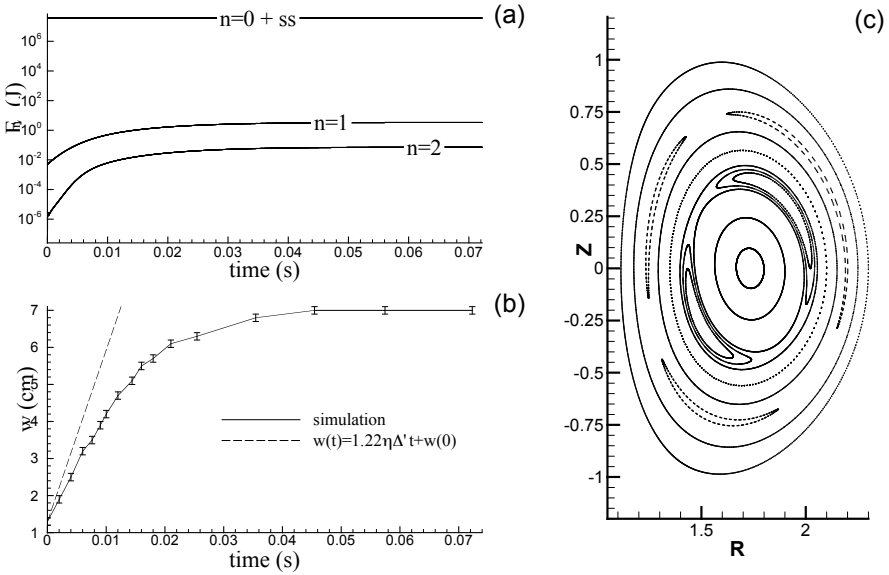

Simulating the slow time-scales of tokamak island evolution is essential for RF/NTM modeling.

Application areas: alternate/emerging concepts

- Integrated MHD and transport modeling of SSPX has been used to study relaxation, transient effects, and reconnection. [longstanding collaboration with B. Cohen and B. Hooper, LLNL; also Held and Ji, USU]
- A new study will assess two-fluid effects in the quiescent spheromak state. [Howell]
- Nonlinear MHD study of PPCD in MST clarifies roles of drive and fluctuation coupling. [Reynolds]
- HIT-II simulation studies CHI for STs reproduce current build-up with flux amplification. [Bayliss, PSI-C support]
- Novel current injection and flux compression schemes in the Pegasus ST are being modeled. [Bayliss and O'Bryan]

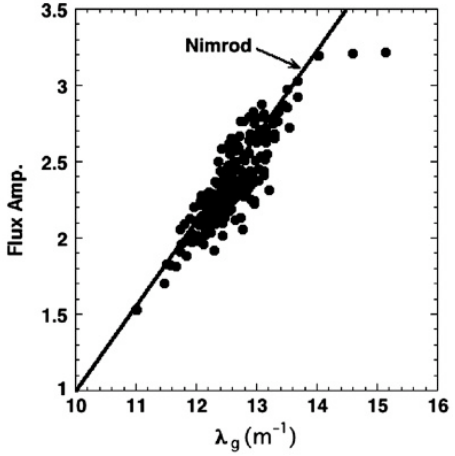

Comparison of results on fluctuation-induced flux amplification from SSPX (dots) and NIMROD simulations (line). [Hooper, et al, NF 47, 1064]

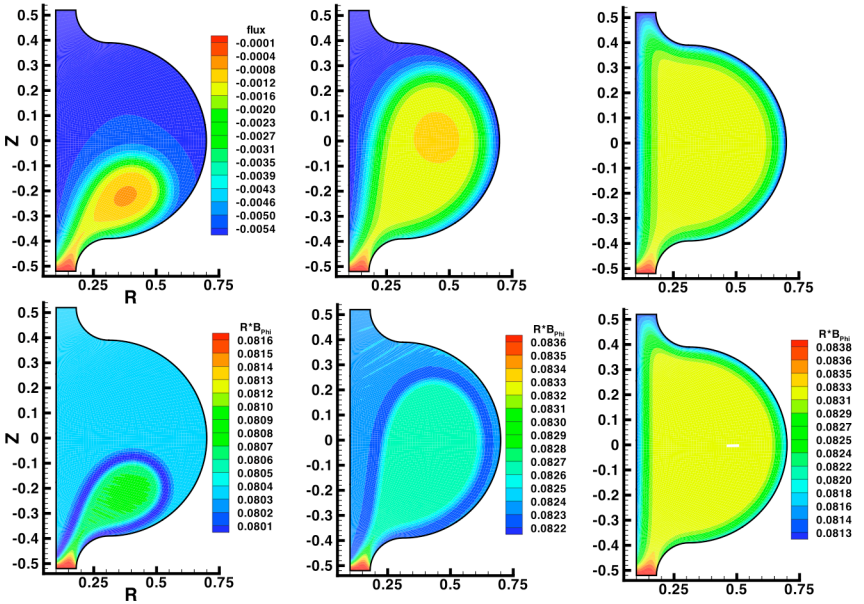

MHD HIT-II simulation sequence of ψ and RB_ϕ.

Application areas: other PSI-Center collaboration

- Two-fluid and MHD studies of FRC spin-up, stability, translation, and RMF current drive. [Milroy and Macnab, U-WA]
- MHD dynamics in Caltech experiment. [Kim, U-WA]
- Current drive in HIT-SI. [Akcay, U-WA]
- New modeling of interchange turbulence in LDX. [Nelson and Kim, U-WA]
- Also support for MBX, PHD, SSX, and TCS. [U-WA]
- Development of graphical interfacing with LLNL's VISIT program. [Nelson, U-WA]

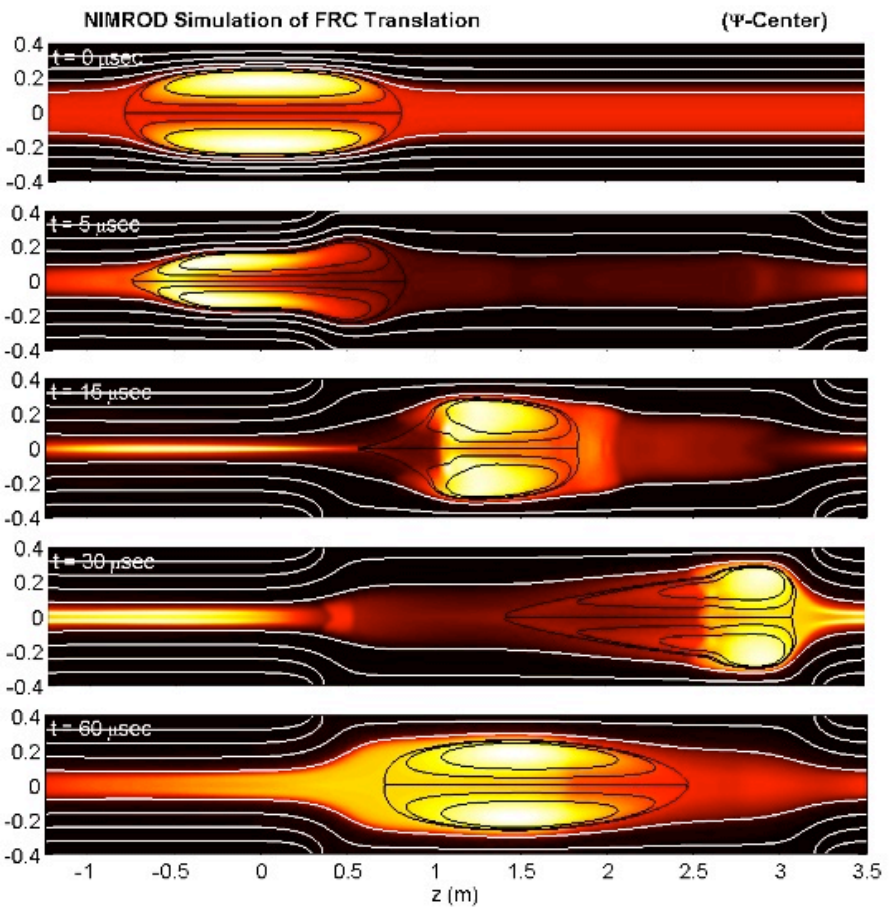

Two-dimensional FRC translation results with MHD modeling--a new OFES research highlight.

Application areas: CMSO-related activities

- Two-fluid modeling of MRX investigates magnetic interaction of reconnection physics and global geometry. [Murphy]
- Astrophysical jet-like configurations investigate collimation, stability, and relaxation. [Carey]

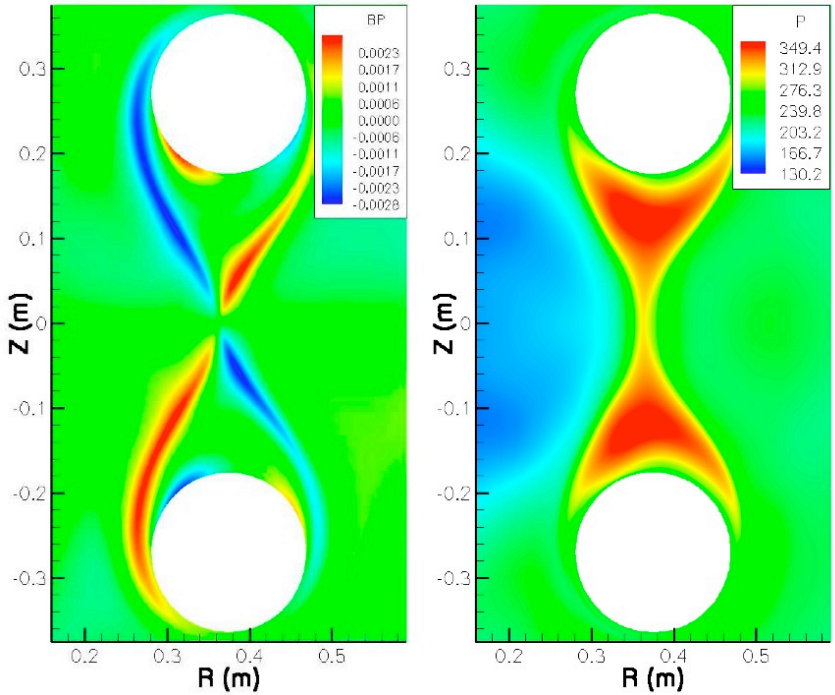

Out-of-plane component of B (left) and pressure (right) from a 2D two-fluid MRX simulation show asymmetry due to geometry.

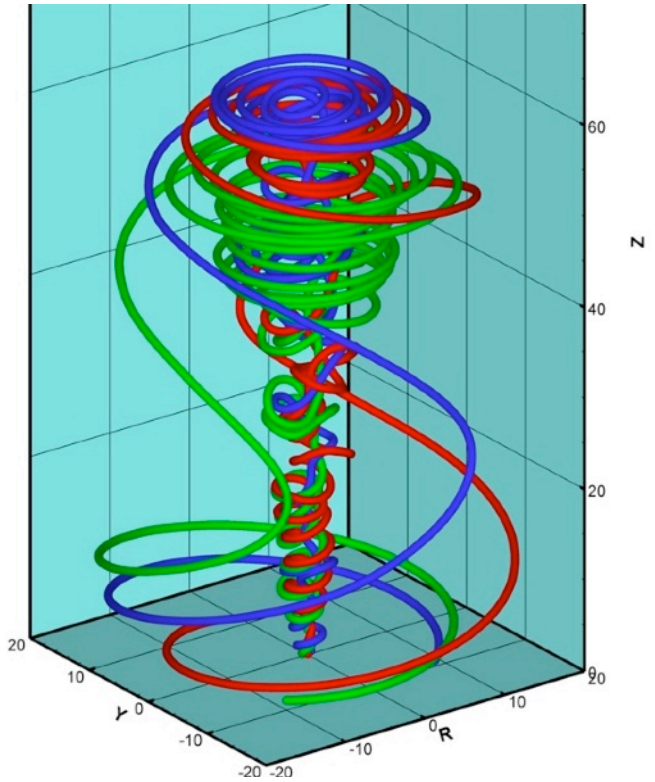

Field-line traces from simulated jet relaxation show topology change from magnetic reconnection.

PDE System: The fluid-based plasma model is related to MHD, but the Hall effect and other two-fluid terms decouple the magnetic field from ion motion at short wavelength.

$$\frac{\partial \mathbf{B}}{\partial t} = -\nabla \times \left(\eta \mathbf{J} - \mathbf{V} \times \mathbf{B} + \frac{1}{ne} \mathbf{J} \times \mathbf{B} - \frac{T}{ne} \nabla n - \frac{1}{ne} \nabla \cdot \Pi_e \right) + \kappa_{divb} \nabla \nabla \cdot \mathbf{B}$$ Faraday's / Ohm's law

$$\mu_0 \mathbf{J} = \nabla \times \mathbf{B}$$ low-ω Ampere's law

$$\rho \left(\frac{\partial \mathbf{V}}{\partial t} + \mathbf{V} \cdot \nabla \mathbf{V} \right) = \mathbf{J} \times \mathbf{B} - \nabla p - \nabla \cdot \Pi_i(\mathbf{V})$$ flow evolution

$$\frac{\partial n}{\partial t} + \nabla \cdot (n \mathbf{V}) = \nabla \cdot D \nabla n$$ particle continuity with artificial diffusivity

$$\frac{n}{\gamma - 1} \left(\frac{\partial T_\alpha}{\partial t} + \mathbf{V}_\alpha \cdot \nabla T_\alpha \right) = -p_\alpha \nabla \cdot \mathbf{V}_\alpha - \nabla \cdot \mathbf{q}_\alpha + Q_\alpha$$ temperature evolution

- The magnetic divergence term and particle diffusion term are used for numerical purposes.
- The implementation of electron stress is under development and will represent the effects of rapid momentum equilibration along magnetic field-lines.

The relations used for $\mathbf{E}$, Π_i, and $\mathbf{q}_\alpha$ determine which theoretical model is solved. [resistive MHD, two-fluid, kinetic effects, etc.]

• Collisional closure relations have limited applicability, but they provide dissipation that is <u>necessary</u> for nonlinear simulations if the algorithm is not inherently dissipative.

Π_i is a combination of Π_{gv}, $\Pi_{||}$, and $\Pi_\perp$

$$\Pi_{gv} = \frac{m_i p_i}{4eB}\left[\hat{\mathbf{b}}\times\mathbf{W}\cdot\left(\mathbf{I}+3\hat{\mathbf{b}}\hat{\mathbf{b}}\right)-\left(\mathbf{I}+3\hat{\mathbf{b}}\hat{\mathbf{b}}\right)\cdot\mathbf{W}\times\hat{\mathbf{b}}\right], \qquad \left(\mathbf{W}\equiv\nabla\mathbf{V}+\nabla\mathbf{V}^{\mathrm{T}}-\frac{2}{3}\mathbf{I}\nabla\cdot\mathbf{V}\right)$$

$$\Pi_{||} = \frac{p_i\tau_i}{2}\left(\hat{\mathbf{b}}\cdot\mathbf{W}\cdot\hat{\mathbf{b}}\right)\left(\mathbf{I}-3\hat{\mathbf{b}}\hat{\mathbf{b}}\right)$$

$$\Pi_\perp \sim -\frac{3p_i m_i^2}{10e^2B^2\tau_i}\mathbf{W} \text{ has been treated as } -nm_i\nu_{iso}\,\mathbf{W} \text{ or } -nm_i\nu_{kin}\,\nabla\mathbf{V}$$

$$\mathbf{q}_i = -n\left[\chi_{||i}\hat{\mathbf{b}}\hat{\mathbf{b}}+\chi_{\perp i}\left(\mathbf{I}-\hat{\mathbf{b}}\hat{\mathbf{b}}\right)\right]\cdot\nabla T_i \;+2.5p_i(eB)^{-1}\hat{\mathbf{b}}\times\nabla T_i$$

$$\mathbf{q}_e = -n\left[\chi_{||e}\hat{\mathbf{b}}\hat{\mathbf{b}}+\chi_{\perp e}\left(\mathbf{I}-\hat{\mathbf{b}}\hat{\mathbf{b}}\right)\right]\cdot\nabla T_e \;-2.5p_e(eB)^{-1}\hat{\mathbf{b}}\times\nabla T_e$$

• Closure terms with local gradients may be treated implicitly and can be used in semi-implicit advances with nonlocal closures. [Held, PoP **11**, 2419 (2004)]

PDE System (continued)

Fluid models of macroscopic MHD activity in MFE plasmas are characterized by extreme stiffness and anisotropy.

- *Stiffness*: Time-scales that impact nonlinear MHD evolution include
  - Parallel particle motion leading to parallel thermal equilibration over flux surfaces in 100s of nanoseconds to microseconds.
  - MHD wave propagation over global scales in microseconds.
  - Magnetic fluctuations and tearing in hundreds of microseconds to milliseconds.
  - Nonlinear profile modification and transport in tens to hundreds of milliseconds.
  - Global resistive diffusion over seconds.
- *Anisotropy*: Magnetization of nearly collisionless particles leads to
  - Effective thermal diffusivity ratios, $\chi_{\|}/\chi_{\perp}$, exceeding 10^{10}.
  - Shear wave resonance that allows nearly singular behavior of MHD modes.

Computational Modeling

Challenges:

- Anisotropy relative to the strong magnetic field
  - Distinct shear and compressive behavior
  - Extremely anisotropic heat flow
- Stiffness arising from multiple time-scales
- Magnetic divergence constraint
- Weak dissipation

Helpful considerations:

- Linear effects impose the time-scale separation
- Typically free of shocks

Modeling: Spatial Representation

• The NIMROD code (http://nimrodteam.org and JCP **195**, 355, 2004) uses finite elements to represent the poloidal plane and finite Fourier series for the periodic direction.

• Polynomial basis functions are Lagrange polynomials with uniform or Gauss-Lobatto-Legendre nodes. Degree>1 provides

- **High-order convergence without uniform meshing**
- **Curved isoparametric mappings**

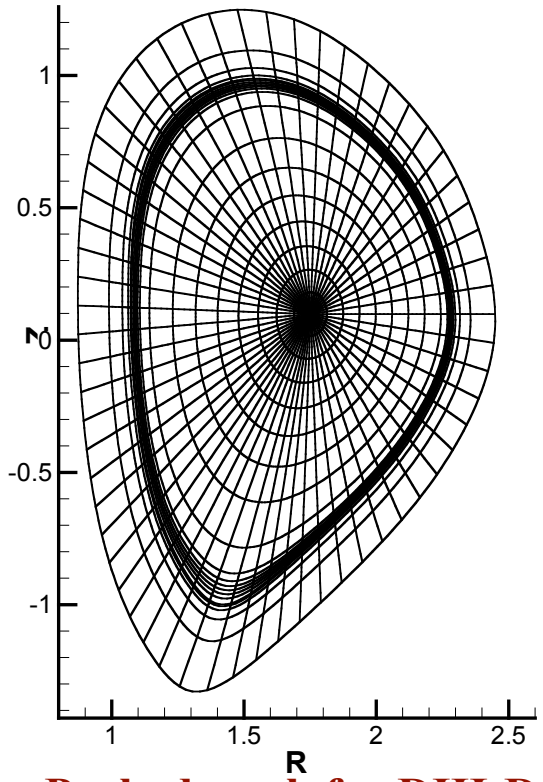

Packed mesh for DIII-D ELM study

SSPX

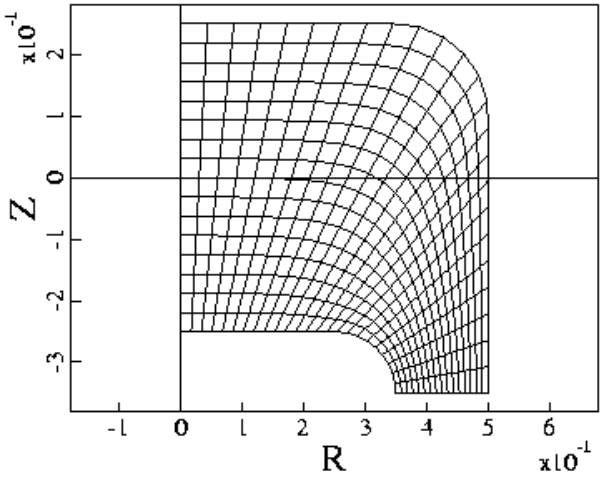

LDX

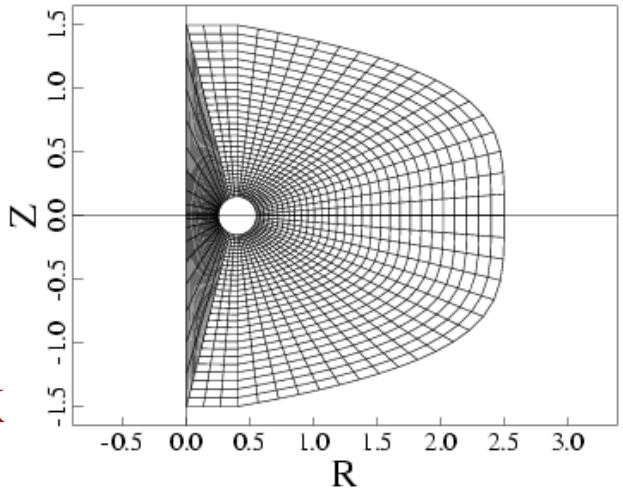

Modeling: Spatial Representation (continued)

- Polynomials of degree>1 also provide
  - **Control of magnetic divergence error**

'Error diffusion' is added to Faraday's law:

$$\frac{\partial \mathbf{B}}{\partial t} = -\nabla \times \mathbf{E} + \kappa_{divb} \nabla \nabla \cdot \mathbf{B}$$

$$\int d\mathbf{x} \left\{ \mathbf{c}* \cdot \Delta \mathbf{b} \; + g \Delta t \, \kappa_{divb} (\nabla \cdot \mathbf{c}*)(\nabla \cdot \Delta \mathbf{b}) \right\}$$

$$= \Delta t \int d\mathbf{x} \left\{ \kappa_{divb} (\nabla \cdot \mathbf{c}*)(\nabla \cdot \mathbf{b}) - (\nabla \times \mathbf{c}*) \cdot \mathbf{E} \right\}$$

$$- \Delta t \oint d\mathbf{s} \times \mathbf{E} \cdot \mathbf{c}*$$

for all vector test functions **c***.

The ratio of DOF/constraints is 3 in the limit of large polynomial degree.

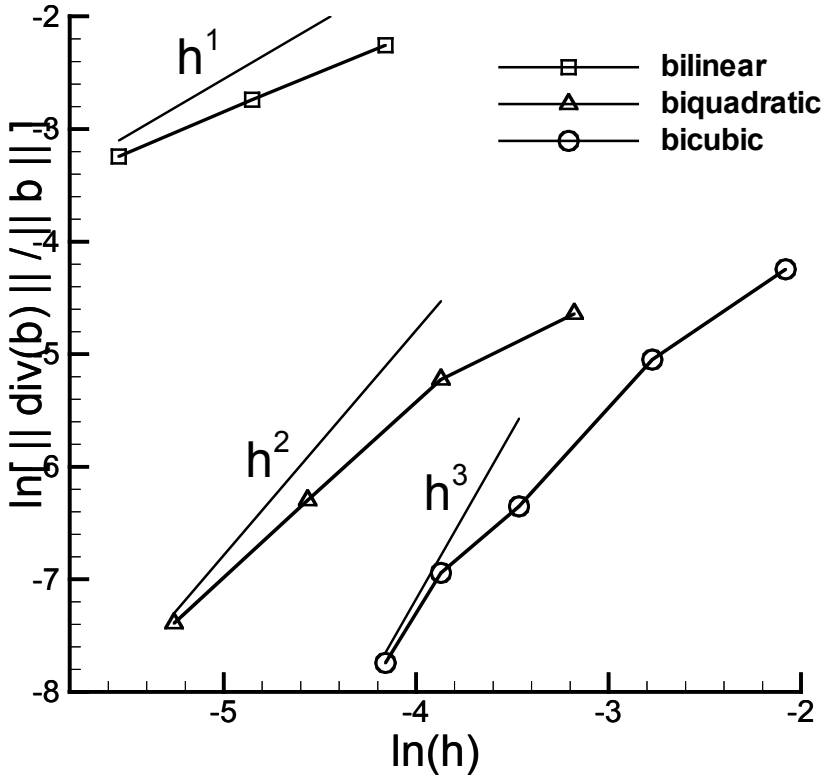

Magnetic divergence errors from a tearing-mode calculation.

Scalings show convergence rates expected for first derivatives.

- Polynomials of degree>1 also provide
  - **Resolution of extreme anisotropies (Lorentz force and diffusion)**

Simple 2D test:

- Homogeneous Dirichlet boundary conditions on T
- Heat and perpendicular current have sources. $2\pi^2 \cos(\pi x)\cos(\pi y)$
- Analytically, the solution is independent of $\chi_{||}$,

$$T(x,y) = \chi_{\perp}^{-1} \cos(\pi x)\cos(\pi y)$$

- The resulting $T^{-1}(0,0)$ measures the effective $\chi_{\perp}$, including the numerical truncation error.

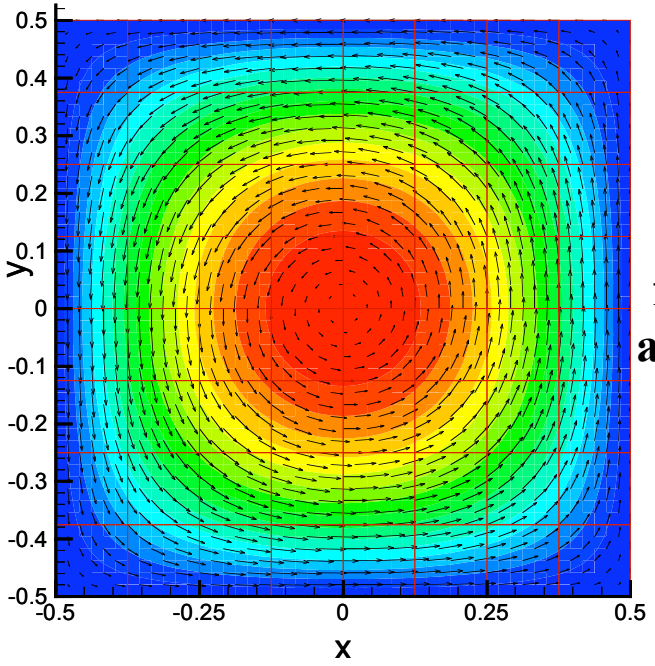

***T* and B fields from an 8×8 mesh of bicubic elements.**

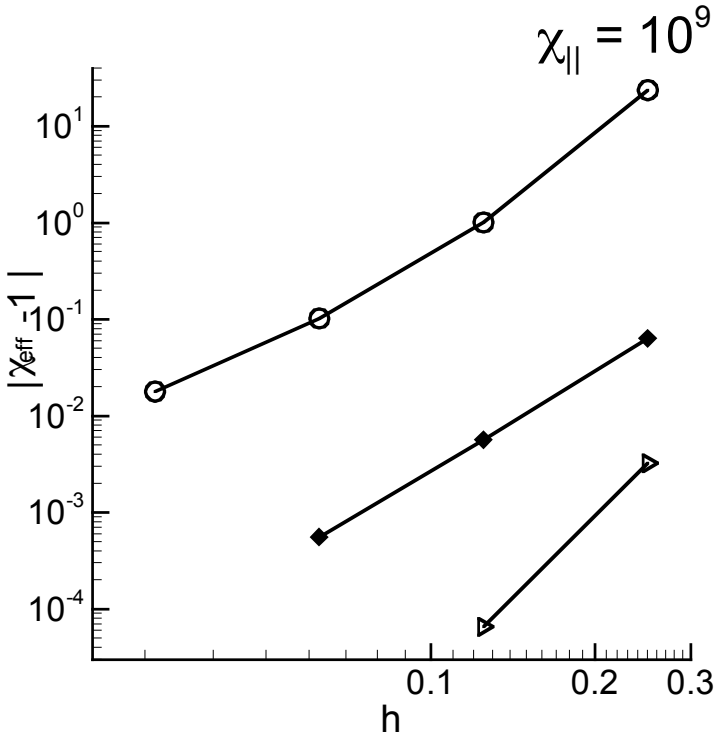

Diffusion error for bicubic, biquartic, and biquintic elements.

Reproducing Transport with Magnetic Islands

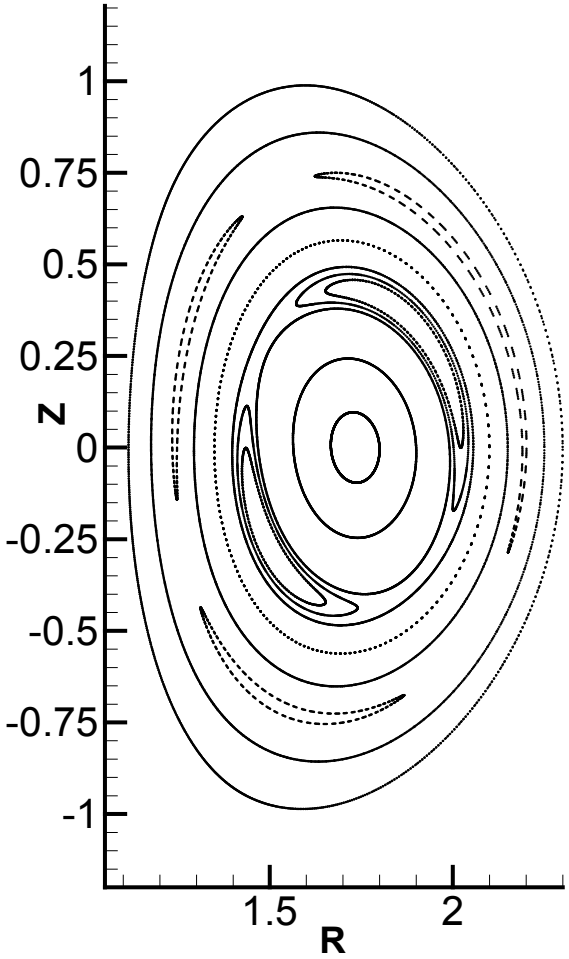

With anisotropy, heat transport across magnetic islands is a competition between parallel and perpendicular processes.

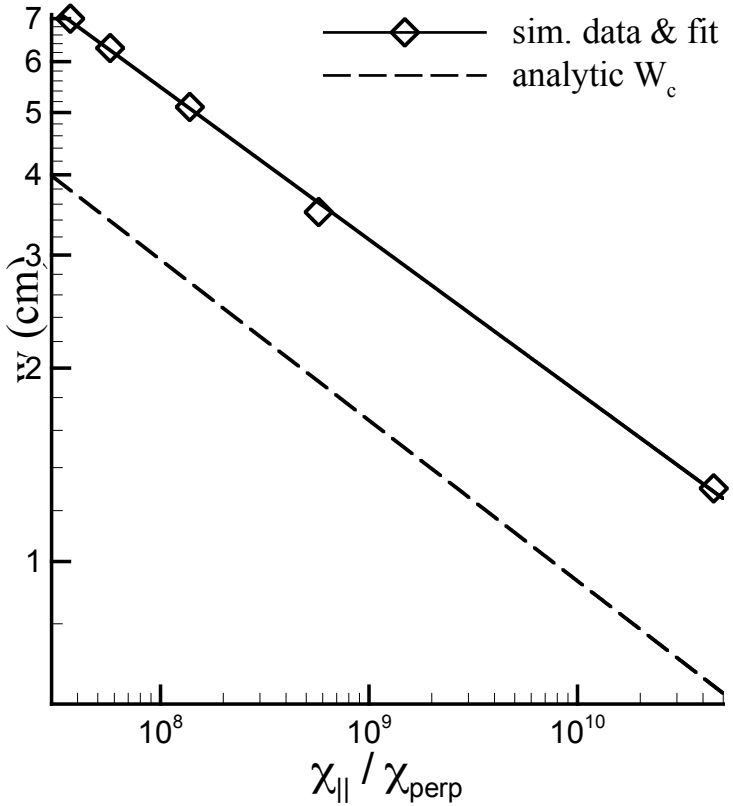

Critical island width vs. $\chi_{||}/\chi_{perp}$
W_c shows where diffusion time-scales match [Fitzpatrick, PoP **2**, 825 (1995)].

Modeling: Time-advance algorithms

- Stiffness from fast parallel transport and wave propagation requires implicit algorithms.
- Semi-implicit methods for MHD have been refined over the last two decades (DEBS, XTOR, NIMROD).
- The underlying scheme is leapfrog,

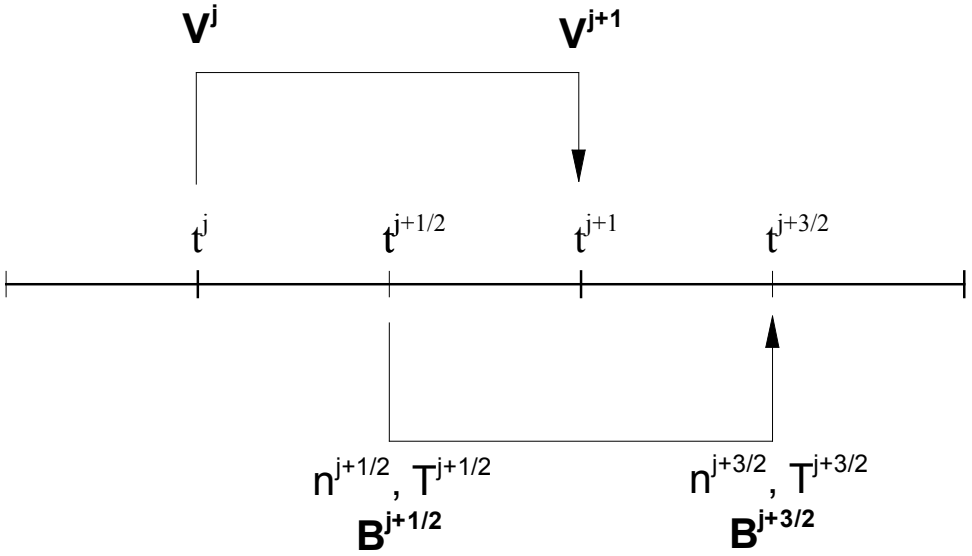

with the following implicit operator in the velocity advance to stabilize waves without numerical dissipation.

$$\mathbf{L}(\Delta\mathbf{V}) = \frac{1}{\mu_0}\left\{\nabla\times\left[\nabla\times\left(\Delta\mathbf{V}\times\mathbf{B}_0\right)\right]\right\}\times\mathbf{B}_0 + \mathbf{J}_0\times\nabla\times\left(\Delta\mathbf{V}\times\mathbf{B}_0\right) + \nabla\left(\Delta\mathbf{V}\cdot\nabla p_0 + \gamma p_0\nabla\cdot\Delta\mathbf{V}\right)$$

Numerical Algorithm: An implicit leapfrog method extends this approach to advance the two-fluid equations.

- The number density appearing in the advances of T and $\mathbf{B}$ is time-averaged, as is the temperature appearing in the magnetic advance.
- A Newton-like computation is used for momentum advection and the Hall term.

$$m_{\mathrm{i}} n^{j+1/2}\left(\frac{\Delta\mathbf{V}}{\Delta t}+\frac{1}{2}\mathbf{V}^{j}\cdot\nabla\Delta\mathbf{V}+\frac{1}{2}\Delta\mathbf{V}\cdot\nabla\mathbf{V}^{j}\right)-\Delta t L^{j+1/2}(\Delta\mathbf{V})+\nabla\cdot\Pi_{\mathrm{i}}(\Delta\mathbf{V})=\mathbf{J}^{j+1/2}\times\mathbf{B}^{j+1/2}$$
$$-m_{\mathrm{i}} n^{j+1/2}\mathbf{V}^{j}\cdot\nabla\mathbf{V}^{j}-\nabla\left[n^{j+1/2}\left(T_e^{j+1/2}+Z^{-1}T_i^{j+1/2}\right)\right]-\nabla\cdot\Pi_{\mathrm{i}}\left(\mathbf{V}^{j}\right)$$

$$\frac{\Delta n}{\Delta t}+\frac{1}{2}\nabla\cdot\left(\mathbf{V}^{j+1}\cdot\Delta n-D\nabla\Delta n\right)=-\nabla\cdot\left(\mathbf{V}^{j+1}\cdot n^{j+1/2}-D\nabla n^{j+1/2}\right)$$

$$\frac{3n}{2}\left(\frac{\Delta T_\alpha}{\Delta t}+\frac{1}{2}\mathbf{V}_\alpha^{j+1}\cdot\nabla\Delta T_\alpha\right)+\frac{n}{2}\Delta T_\alpha\nabla\cdot\mathbf{V}_\alpha^{j+1}+\frac{1}{2}\nabla\cdot\mathbf{q}_\alpha(\Delta T_\alpha)$$
$$=-\frac{3n}{2}\mathbf{V}_\alpha^{j+1}\cdot\nabla T_\alpha^{j+1/2}-nT_\alpha^{j+1/2}\nabla\cdot\mathbf{V}_\alpha^{j+1}\ -\nabla\cdot\mathbf{q}_\alpha\left(T_\alpha^{j+1/2}\right)+Q_\alpha^{j+1/2}$$

$$\frac{\Delta\mathbf{B}}{\Delta t}-\frac{1}{2}\nabla\times\left(\mathbf{V}^{j+1}\times\Delta\mathbf{B}\right)+\frac{1}{2}\nabla\times\frac{1}{ne}\left(\mathbf{J}^{j+1/2}\times\Delta\mathbf{B}+\Delta\mathbf{J}\times\mathbf{B}^{j+1/2}\right)+\frac{1}{2}\nabla\times\eta\Delta\mathbf{J}$$
$$=-\nabla\times\left[\frac{1}{ne}\left(\mathbf{J}^{j+1/2}\times\mathbf{B}^{j+1/2}-T_e\nabla n\right)-\mathbf{V}^{j+1}\times\mathbf{B}^{j+1/2}+\eta\mathbf{J}^{j+1/2}\right]$$

- A corrector step for temperature is used for **B**- or T-dependent thermal conduction.

Analysis of the linearized difference equations shows that the implicit leapfrog is numerically stable and accurate on two-fluid waves.

- Real (top) and imaginary (bottom) parts of computed frequencies for $\Delta t\ \Omega_i = 1$ and $c_s^2/v_A^2 = 0.1$.
- Numerical dispersion is apparent for wavelengths near the ion skin depth.
- Roundoff level imaginary frequencies prove absence of numerical dissipation.

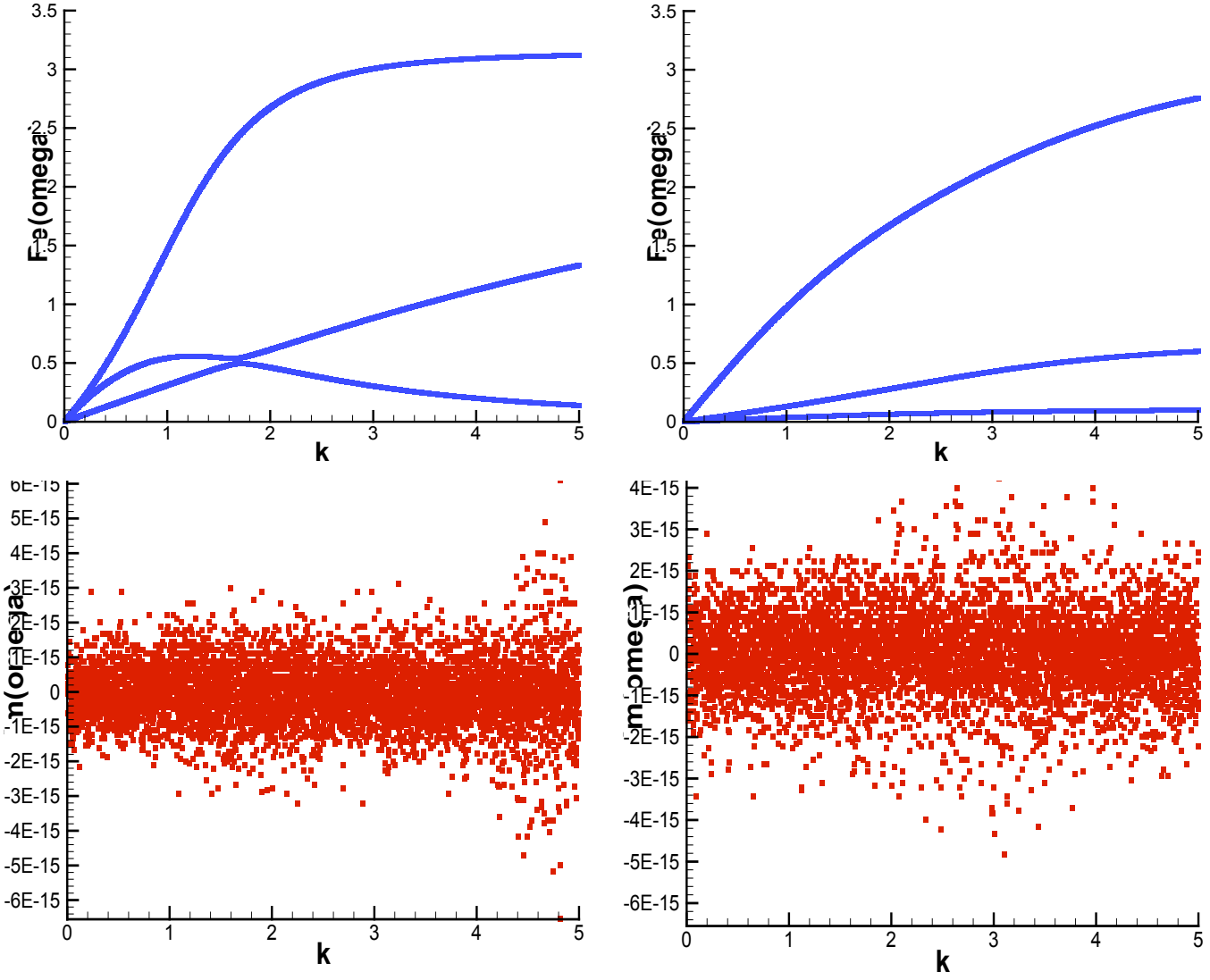

Parallel propagation: $\theta = 0.04\pi$

Perpendicular propagation: $\theta = 0.46\pi$

Comparing IL with time-centered, IL shows more numerical dispersion in the cyclotron resonance and slightly less in the whistler wave for $\Delta t\ \Omega_i > 0.5$.

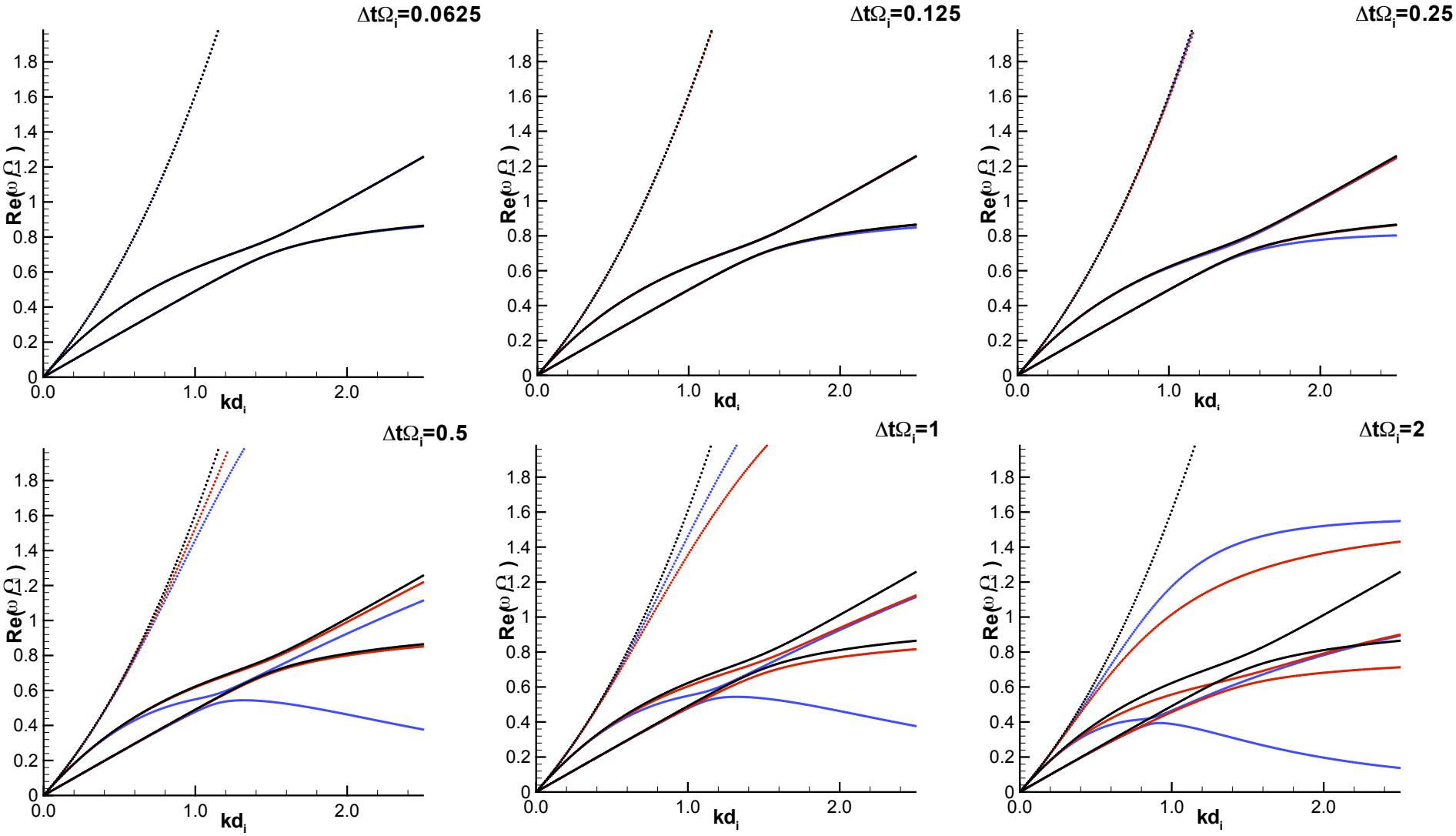

$\theta = 0.04\pi$ HMHD Leapfrog Time-centered

There is less to distinguish the two algorithms for nearly perpendicular propagation, except that time-centered has better accuracy for the KAW.

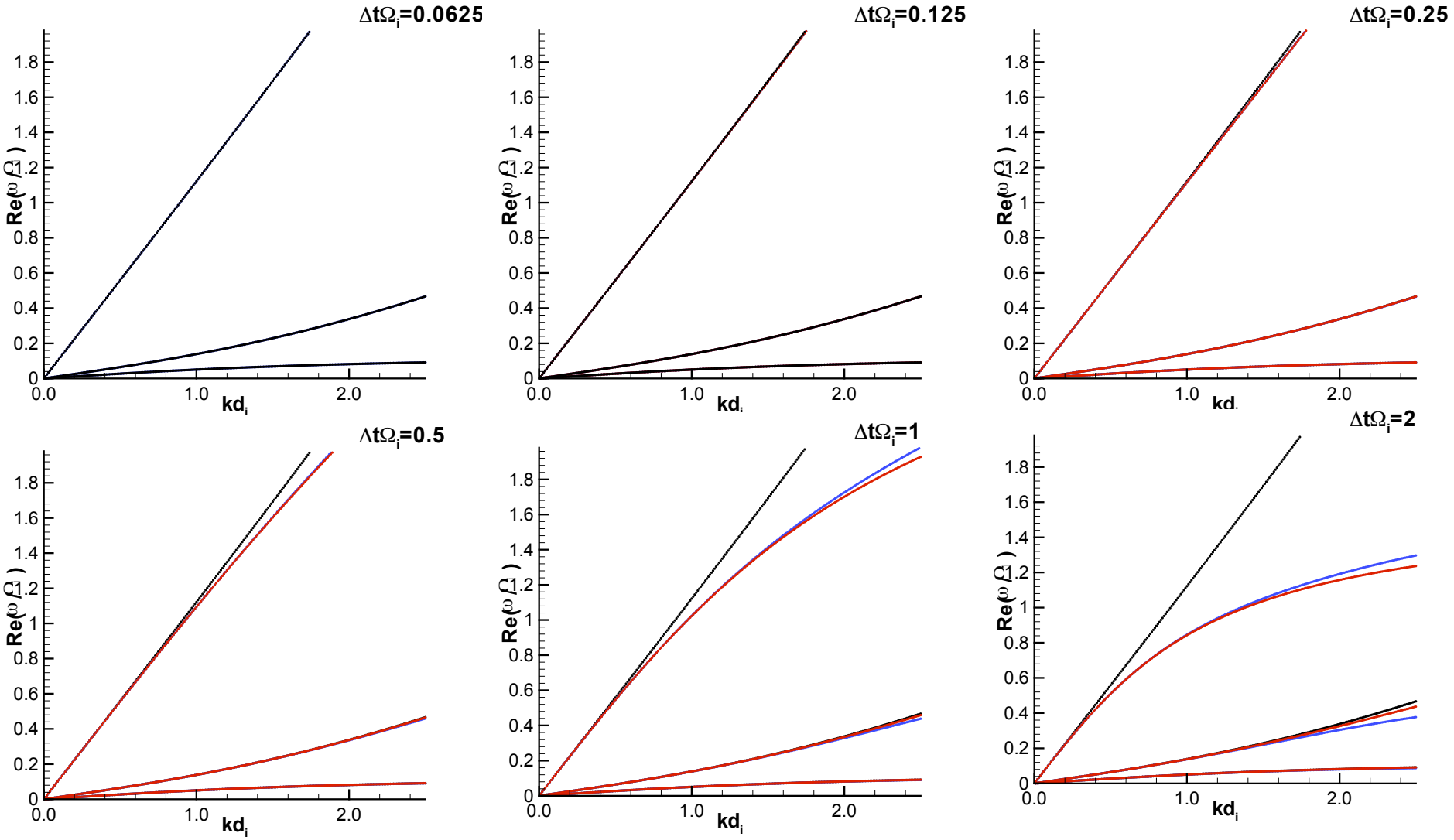

$\theta = 0.46\pi$ HMHD Leapfrog Time-centered

Implementation: Algebraic systems from 2D and 3D operations are solved during each time-step (~10,000s over a nonlinear simulation).

- 3D systems result from nonlinear fluctuations in toroidal angle.
  - Toroidal couplings are computed with FFTs in matrix-free solves.
- 2D systems represent coupling over the FE mesh only, and matrix elements are computed.
  - They are also generated for preconditioning the matrix-free solves.

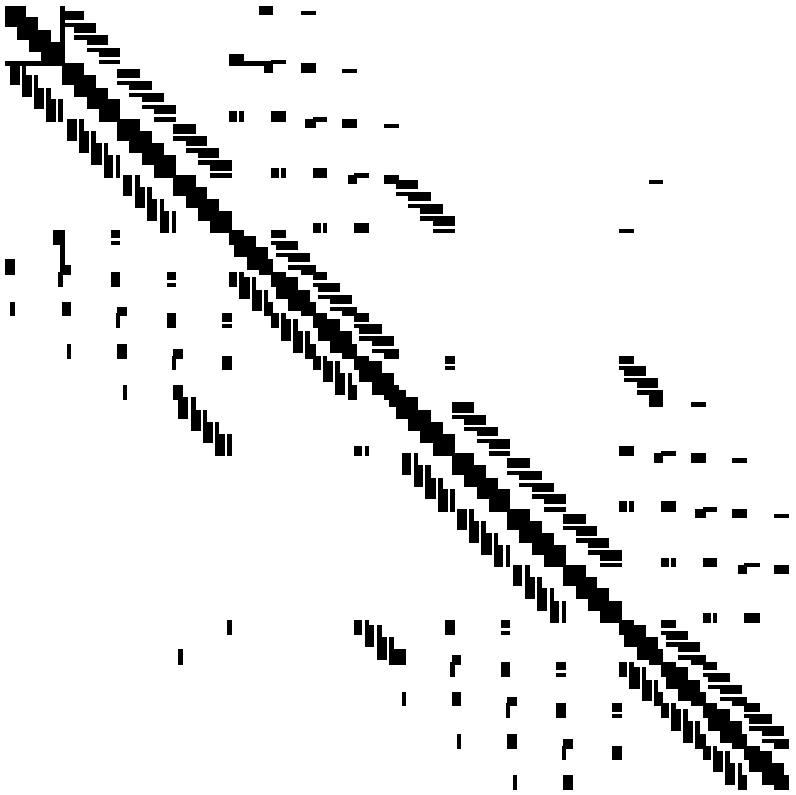

Example sparsity pattern for a small mesh of biquartic elements—after static condensation but before reordering.

Solving algebraic systems dominates computation time.

- Iterative methods scale well but tend to perform poorly on ill-conditioned systems.
- Collaborations with **TOPS** Center researchers Kaushik and Li led us to parallel direct methods with reordering→SuperLU (http://crd.lbl.gov/~xiaoye/SuperLU/).
- For our nonlinear MHD computations, preconditioning based on direct solves of the coupling over the poloidal plane is sufficient.

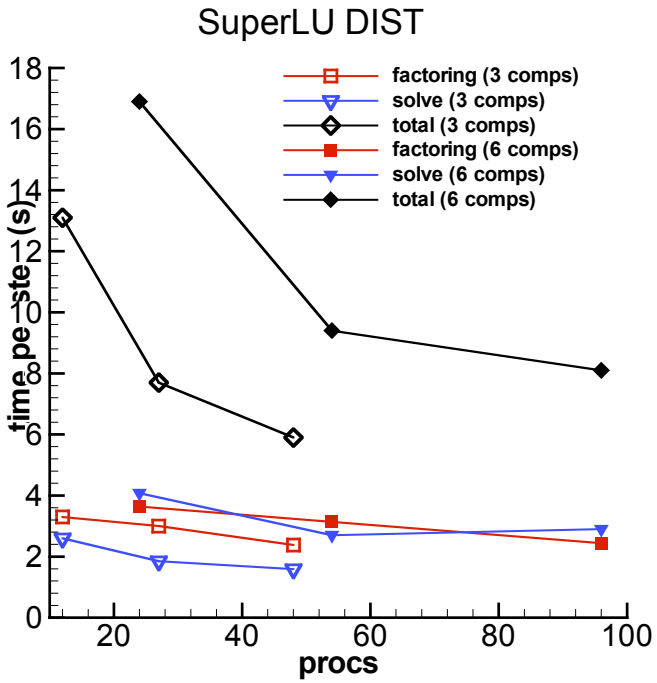

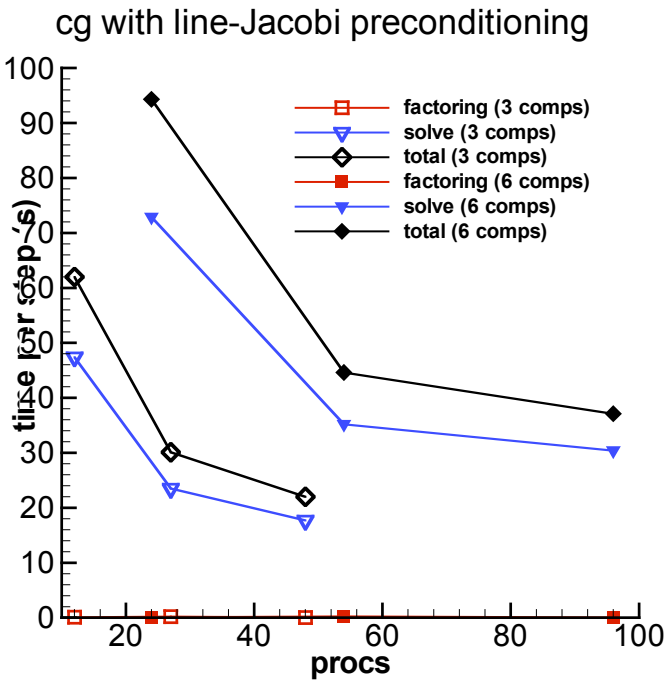

SuperLU improves NIMROD performance by a factor of 5 in nonlinear MHD simulations.

- Nonlinear computations with the two-fluid model seem to require preconditioning that also accounts for toroidal coupling.

Conclusions

The challenges of macroscopic plasma modeling are being met by developments in numerical and computational techniques, as well as advances in hardware.

- High-order spatial representation controls magnetic divergence error and allows resolution of anisotropies that were previously considered beyond reach.
- A new implicit leapfrog method has been developed and analyzed for the two-fluid system.
- SciDAC-fostered collaborations have resulted in significant performance gains through sparse parallel direct solves (with SuperLU).

At the same time, the project has maintained an emphasis on applications and helping non-developers learn to use the code.

- Development activities have been prioritized for applications.
- The emphasis on current applications needs to continue through the new era of integrated modeling.